

Actinide Hydride Complexes as Multielectron Reductants: Analogous Reduction Chemistry from $[(C_5Me_5)_2UH]_2$, $[(C_5Me_5)_2UH_2]_2$, and $[(C_5Me_5)_2ThH_2]_2$

William J. Evans,^{*,†} Kevin A. Miller,[†] Stosh A. Kozimor,[†] Joseph W. Ziller,[†]
Antonio G. DiPasquale,[‡] and Arnold L. Rheingold[‡]

Department of Chemistry, University of California Irvine, California 92697-2025, and Department of
Chemistry and Biochemistry, University of California, San Diego, 9500 Gilman Drive, MC 0358,
La Jolla, California 92093-0358

Received April 4, 2007

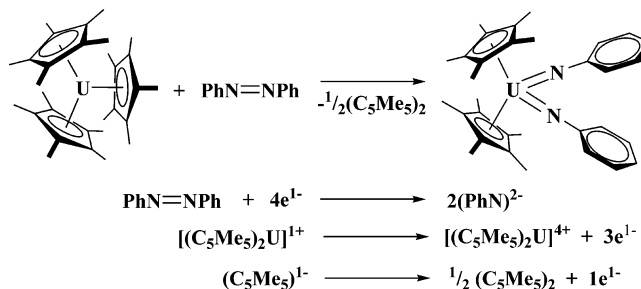
Methods to separate the components of the equilibrium mixture of $[(C_5Me_5)_2UH]_2$ and $[(C_5Me_5)_2UH_2]_2$ have been developed that allow their reductive chemistry to be studied. These actinide hydrides can act as four-, six-, and eight-electron reductants depending on the substrate with H_2 as the byproduct of a $H^- \rightarrow e^- + \frac{1}{2} H_2$ redox couple. This hydride reduction chemistry allows complexes of redox-inactive Th^{4+} such as $[(C_5Me_5)_2ThH_2]_2$ to be four- and six-electron reductants. $[(C_5Me_5)_2UH]_2$ and $[(C_5Me_5)_2UH_2]_2$ cleanly reduce 2 equiv of $PhEPh$ ($E = S, Se$) to form 2 equiv of $(C_5Me_5)_2U(SPh)_2$ and $(C_5Me_5)_2U(SePh)_2$ in an overall four-electron reduction in each case. $[(C_5Me_5)_2UH]_2$ and $[(C_5Me_5)_2UH_2]_2$ also effect a six-electron reduction of 3 equiv of 1,3,5,7-cyclooctatetraene to $[(C_5Me_5)(C_8H_8)U]_2$ (C_8H_8) and an eight-electron reduction of 2 equiv of $PhN=NPh$ to form 2 equiv of the U^{6+} imido complex $(C_5Me_5)_2U(=NPh)_2$. In each reaction, H_2 is a byproduct. This hydride-based reduction is also successful with the tetravalent thorium hydride $[(C_5Me_5)_2ThH_2]_2$, which reduces 2 equiv of $PhSPh$ to $(C_5Me_5)_2Th(SPh)_2$ and 3 equiv of C_8H_8 to $[(C_5Me_5)(C_8H_8)Th]_2(C_8H_8)$ with concomitant formation of H_2 . X-ray crystallographic data are reported on $[(C_5Me_5)_2UH]_2$, $[(C_5Me_5)_2UH_2]_2$, and $(C_5Me_5)_2U(SePh)_2$ as well as the thorium reduction products $(C_5Me_5)_2Th(SPh)_2$ and $[(C_5Me_5)(C_8H_8)Th]_2(C_8H_8)$.

Introduction

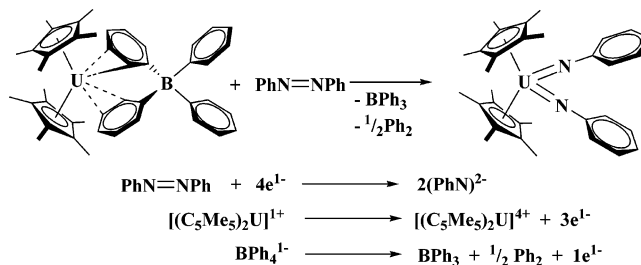
Recent studies of the sterically crowded organoactinide complex $(C_5Me_5)_3U^I$ have shown that it can function as a multielectron reductant by combining its traditional U^{3+} reductive chemistry^{2–4} with $(C_5Me_5)^-$ -based reduction.^{5,6} This type of ligand-based reduction is called sterically induced reduction since it occurs only in complexes with unusually long metal–ligand bonds.⁷ For example, a four-electron reduction can be effected using 1 equiv of U^{3+} and a $(C_5Me_5)^-/(C_5Me_5)$ transformation,⁵ Scheme 1. Sterically crowded $[(C_5Me_5)_2U]_2$ - (C_6H_6) ⁸ reacts similarly.⁶

As a control reaction for this sterically induced reduction chemistry, $[(C_5Me_5)_2U][(\mu-Ph)_2BPh_2]$,⁹ a complex that has normal bond lengths, was treated with $PhN=NPh$ for comparison.⁶ Surprisingly, the same four-electron reduction shown in Scheme 1 occurred as shown in Scheme 2. In this case the U^{3+} reduction was combined with a $(BPh_4)^-$ -based reduction that

Scheme 1



Scheme 2



did not require steric crowding. Ligand- and metal-based multielectron reduction have also been observed with $\{[(tBu)-(C_6H_3Me_2-3,5)N]_2U\}(C_6H_5Me)$,¹⁰ another complex that has conventional bond distances.

To explore the potential for other multielectron reduction reactions using ligand-based processes in U^{3+} complexes with

* Corresponding author. Fax: 949-824-2210. E-mail: wevans@uci.edu.

[†] University of California Irvine.

[‡] University of California, San Diego.

(1) Evans, W. J.; Forrestal, K. J.; Ziller, J. W. *Angew. Chem., Int. Ed.* **1997**, *36*, 774.

(2) Evans, W. J.; Kozimor, S. A. *Coord. Chem. Rev.* **2006**, *250*, 911.

(3) Castro-Rodriguez, I.; Meyer, K. *Chem. Commun.* **2006**, 1353.

(4) Ephritikhine, M. *Dalton Trans.* **2006**, 2501.

(5) Evans, W. J.; Nyce, G. W.; Ziller, J. W. *Angew. Chem., Int. Ed.* **2000**, *39*, 240.

(6) Evans, W. J.; Kozimor, S. A.; Ziller, J. W. *Chem. Commun.* **2005**, 4681.

(7) Evans, W. J. *Coord. Chem. Rev.* **2000**, *206–207*, 263.

(8) Evans, W. J.; Kozimor, S. A.; Ziller, J. W.; Kaltsoyannis, N. *J. Am. Chem. Soc.* **2004**, *126*, 14533.

(9) Evans, W. J.; Nyce, G. W.; Forrestal, K. J.; Ziller, J. W. *Organometallics* **2002**, *21*, 1055.

(10) Diaconescu, P. L.; Arnold, P. L.; Baker, T. A.; Mindiola, D. J.; Cummins, C. C. *J. Am. Chem. Soc.* **2000**, *122*, 6108.

Table 1. X-ray Data Collection Parameters for [(C₅Me₅)₂UH]₂, **1**, [(C₅Me₅)₂UH₂]₂, **2**, (C₅Me₅)₂U(SePh)₂, **5**, (C₅Me₅)₂Th(SPh)₂, **8**, and [(C₅Me₅)(C₈H₈)Th]₂(C₈H₈), **9**

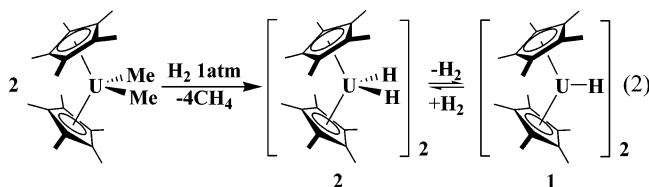
| | | | | | |
|---|--|--|---|---|---|
| empirical formula | C ₄₀ H ₆₂ U ₂ ·(C ₇ H ₈) | C ₄₀ H ₆₄ U ₂ | C ₃₂ H ₄₀ Se ₂ U | C ₃₂ H ₄₀ S ₂ Th | C ₄₄ H ₅₄ Th ₂ ·(C ₆ H ₆) |
| fw | 1111.09 | 1020.99 | 820.59 | 720.80 | 1125.06 |
| temperature (K) | 163(2) | 208(2) | 100(2) | 168(2) | 163(2) |
| cryst syst | monoclinic | monoclinic | hexagonal | hexagonal | monoclinic |
| space group | P2 ₁ /n | C2/c | P6 ₁ | P6 ₅ | C2 |
| a (Å) | 16.032(2) | 18.8970(1) | 12.7763(6) | 12.6647(6) | 15.372(7) |
| b (Å) | 14.186(2) | 12.8770(7) | 12.7763(6) | 12.6647(6) | 9.907(4) |
| c (Å) | 38.211(6) | 16.2190(9) | 32.1519(19) | 32.450(3) | 13.781(6) |
| α (deg) | 90 | 90 | 90 | 90 | 90 |
| β (deg) | 96.765(3) | 104.8110(10) | 90 | 90 | 103.242(7) |
| γ (deg) | 90 | 90 | 120 | 120 | 90 |
| volume (Å ³) | 8630(2) | 3815.5(4) | 4545.1(4) | 4507.5(5) | 2042.9(15) |
| Z | 8 | 4 | 6 | 6 | 2 |
| ρ _{calcd} (Mg/m ³) | 1.710 | 1.774 | 1.799 | 1.593 | 1.829 |
| μ (mm ⁻¹) | 7.526 | 8.502 | 7.777 | 5.119 | 7.305 |
| R1 [I > 2.0σ(I)] ^a | 0.0460 | 0.0477 | 0.0267 | 0.0235 | 0.0273 |
| wR2 (all data) ^a | 0.1054 | 0.1225 | 0.0467 | 0.0462 | 0.0716 |

^a Definitions: wR2 = [Σ[w(F_o² - F_c²)/Σ[w(F_o²)]]^{1/2}, R1 = Σ||F_o - |F_c||/Σ|F_o|.

normal bond lengths, the reductive chemistry of [(C₅Me₅)₂UH]₂, **1**, was of interest. Hydrides are well-known reductants, but they generally add to the substrate during the reduction.¹¹ Since the f element hydrides are primarily known for insertion and σ bond metathesis reactivity,^{12–14} a reduction reaction of the type shown in eq 1 analogous to the ligand-based reductions in Scheme 1



and **2** would not be a traditional reaction for these complexes. In addition, the use of [(C₅Me₅)₂UH]₂, **1**, was complicated by the fact that this trivalent hydride typically exists as an equilibrium mixture with the tetravalent hydride [(C₅Me₅)₂-UH₂]₂, **2**, eq 2.¹⁵



Reported here are conditions in which trivalent **1** can be isolated from tetravalent **2** such that the reduction chemistry of each can be examined with several different classes of substrates: PhEPh (E = S, Se), 1,3,5,7-cyclooctatetraene, and PhN=NPh. Encouraged by the reduction chemistry observed with these organometallic uranium hydrides, extension of this ligand-based hydride chemistry to thorium was examined.

Reduction chemistry with organometallic thorium complexes has traditionally been challenging because only three organometallic Th³⁺ compounds have been fully characterized,¹⁶ [(RMe₂Si)₂C₅H₃]₃Th (R = Me, ^tBu)^{17,18} and {[(^tBuMe₂Si)₂C₈H₆]₂-Th}K(DME)₂.¹⁹ Reduction reactions with thorium have typically

involved addition of external reductants such as alkali metal naphthalides.^{16,20–24} As described here, the tetravalent thorium hydride, [(C₅Me₅)₂ThH₂]₂,^{15,25} **3**, is also an excellent reductant and can achieve multielectron reduction reactivity analogous to that of tetravalent and trivalent uranium hydrides.

Experimental Section

The manipulations described below were performed under argon with rigorous exclusion of air and water using Schlenk, vacuum line, and glovebox techniques. Solvents were dried over Q-5 and molecular sieves and saturated with argon using GlassContour²⁶ columns. Toluene-*d*₈ and benzene-*d*₆ were dried over NaK alloy and vacuum transferred before use. (C₅Me₅)₂ThCl₂,¹⁵ (C₅Me₅)₂-UMe₂,¹⁵ [(C₅Me₅)₂UH₂]₂,¹⁵ [(C₅Me₅)₂ThH₂]₂,¹⁵ and KSPH²⁷ were prepared as previously described. PhSSPh, PhSeSePh, and PhN=NPh were purchased from Aldrich and sublimed before use. 1,3,5,7-C₈H₈ was distilled onto molecular sieves before use. NMR spectra were recorded with a Bruker DRX 500 MHz system. Infrared spectra were recorded as either thin films obtained from C₆H₆ on an ASI ReactIR 1000 instrument²⁸ or as KBr pellets on a Perkin-Elmer Spectrum One FT-IR spectrometer. Elemental analyses were performed by Analytische Laboratorien, Lindlar, Germany. X-ray data collection parameters are given in Table 1, and full crystallographic information is in the Supporting Information.

Crystallization of [(C₅Me₅)₂UH]₂, **1.** A flask fitted with a high-vacuum greaseless stopcock was charged with a solution of (C₅-Me₅)₂UMe₂ (100 mg, 0.186 mmol) in benzene (15 mL). The flask was attached to a high-vacuum line (1 × 10⁻⁵ Torr) and degassed by three freeze–pump–thaw cycles. H₂ (1 atm) was introduced into the flask at room temperature. The red solution slowly changed to brown-green as it was stirred for 12 h. The brown-green solid

(19) Parry, J. S.; Cloke, F. G. N.; Coles, S. J.; Hursthouse, M. B. *J. Am. Chem. Soc.* **1999**, *121*, 6867.

(20) Korobkov, I.; Gambarotta, S.; Yap, G. P. A. *Angew. Chem., Int. Ed.* **2003**, *42*, 814.

(21) Korobkov, I.; Gambarotta, S.; Yap, G. P. A. *Angew. Chem., Int. Ed.* **2003**, *42*, 4958.

(22) Korobkov, I.; Arunachalampillai, A.; Gambarotta, S. *Organometallics* **2004**, *23*, 6248.

(23) Korobkov, I.; Gambarotta, S. *Organometallics* **2004**, *23*, 5379.

(24) Arunachalampillai, A.; Gambarotta, S.; Korobkov, I. *Organometallics* **2005**, *24*, 1996.

(25) Broach, R. W.; Schultz, A. J.; Williams, J. M.; Brown, G. M.; Manriquez, J. M.; Fagan, P. J.; Marks, T. J. *Science* **1979**, *203*, 172.

(26) For more information on drying systems, see www.glasscontour.com

(27) Evans, W. J.; Miller, K. A.; Lee, D. S.; Ziller, J. W. *Inorg. Chem.* **2005**, *44*, 4326.

(28) Evans, W. J.; Johnston, M. A.; Ziller, J. W. *Inorg. Chem.* **2000**, *39*, 3421.

(11) James, B. R. In *Comprehensive Organometallic Chemistry*; Wilkinson, G.; Gordon, F.; Stone, A.; Abel, E. W., Eds.; Peragon: Oxford, 1982; Chapter 51.

(12) Marks, T. J.; Lin, Z. *J. Am. Chem. Soc.* **1987**, *109*, 7979.

(13) Marks, T. J.; Lin, Z. *J. Am. Chem. Soc.* **1990**, *112*, 5515.

(14) Ephritikhine, M. *Chem. Rev.* **1997**, *97*, 2193.

(15) Marks, T. J.; Fagan, P. J.; Manriquez, J. M.; Maatta, E. A.; Seyam, A. M. *J. Am. Chem. Soc.* **1981**, *103*, 6650.

(16) Arunachalampillai, A.; Crewdson, P.; Korobkov, I.; Gambarotta, S. *Organometallics* **2006**, *25*, 3856.

(17) Blake, P. C.; Lappert, M. F.; Atwood, J. L.; Zhang, H. *J. Chem. Soc., Chem Commun.* **1986**, 1148.

(18) Blake, P. C.; Edelstein, N. M.; Hitchcock, P. B.; Kot, W. K.; Lappert, M. F.; Shalimoff, G. V.; Tian, S. *J. Organomet. Chem.* **2001**, *636*, 124.

was extracted with hexane in an argon-filled glovebox and centrifuged to remove brown solids. The hexane solution was stirred for 3 h, the hexane was removed under vacuum, toluene was added, the solution was stirred for 1 h, and the toluene was removed under vacuum, yielding a brown-green powder. ^1H NMR analysis was consistent with the formation of previously reported $[(\text{C}_5\text{Me}_5)_2\text{UH}]_2$,¹⁵ although a small amount of $[(\text{C}_5\text{Me}_5)_2\text{UH}_2]_2$ ¹⁵ was also present (15:1 by ^1H NMR spectroscopy). Black polyhedral crystals suitable for X-ray diffraction were grown at -35°C after 2 days from a saturated solution of **1** in toluene.

Crystallization of $[(\text{C}_5\text{Me}_5)_2\text{UH}]_2$, **2.** Addition of 4 mL of hot hexane and 4 mL of hot toluene to $(\text{C}_5\text{Me}_5)_2\text{UMe}_2$ (668 mg, 1.25 mmol) produced a saturated red solution that was transferred to a Fisher Porter high-pressure reaction vessel. This was degassed to the vapor pressure of the solvent and pressurized to 80 psi with H_2 . After 2 days, large black crystalline rods formed. The pressure was reduced to 20 psi, the reaction vessel was brought into the argon glovebox, and the vessel was evacuated to the vapor pressure of the solvent and backfilled with argon ($3\times$). The solvent was decanted to leave black crystals that analyzed by ^1H NMR and IR spectroscopy to be $[(\text{C}_5\text{Me}_5)_2\text{UH}_2]_2$.¹⁵

$(\text{C}_5\text{Me}_5)_2\text{U}(\text{SPh})_2$, **4.** PhSSPh (12 mg, 0.055 mmol) in C_6D_6 was added to a J-Young tube containing **1** (29 mg, 0.028 mmol) in C_6D_6 . The J-Young tube was capped immediately, and a color change from brown to red was observed along with the formation of bubbles. ^1H NMR spectroscopy showed quantitative conversion of starting material to the previously characterized **4**²⁹ and H_2 exhibiting a ^1H NMR resonance at 4.46 ppm.

$(\text{C}_5\text{Me}_5)_2\text{U}(\text{SePh})_2$, **5.** PhSeSePh (75 mg, 0.240 mmol) in toluene (3 mL) was added to a brown-green solution of **1** (122 mg, 0.120 mmol) in toluene (10 mL). A dark red solution immediately formed and bubbles were observed. After the mixture was stirred for 12 h, the dark orange solution was evaporated to dryness, yielding a red oil. The red oil was dissolved in hexane and cooled to -35°C . After 2 days, **5** was obtained as red crystals (132 mg, 67%). Crystals of **5** suitable for X-ray diffraction were grown at -35°C from a concentrated hexane solution. ^1H NMR (C_6D_6): δ 14.0 (s, 30H C_5Me_5 , $\Delta\nu_{1/2} = 18$ Hz), 2.6 (t, 2H, $^3J_{\text{HH}} = 8$ Hz, *p*-H), -31.0 (br s, 4H, $\Delta\nu_{1/2} = 28$ Hz, *m*-H), 0.98 (d, 4H, $^3J_{\text{HH}} = 8$ Hz, *o*-H). ^{13}C NMR (C_6D_6): δ -25.6 (C_5Me_5), 126.0 (C_5Me_5), 104.5 (*o*-phenyl), 159.7 (*m*-phenyl), 134.2 (*p*-phenyl), 129.7 (*ipso*-phenyl). IR (thin film): 3053w, 2964m, 2907m, 2856m, 1575m, 1476m, 1436s, 1378m, 1325w, 1297w, 1262vs, 1089s, 1015vs, 865w, 799s, 773s, 691s, 664s cm^{-1} . Anal. Calcd for $\text{C}_{32}\text{H}_{40}\text{Se}_2\text{U}$: C, 46.84; H, 4.91; Se, 19.24; U, 29.01. Found: C, 46.88; H, 5.05; Se, 19.41; U, 28.80.

$[(\text{C}_5\text{Me}_5)(\text{C}_8\text{H}_8)\text{U}]_2(\text{C}_8\text{H}_8)$, **6.** 1,3,5,7- C_8H_8 (9.8 μL , 0.087 mmol) in C_6D_6 was added to a J-Young tube containing $[(\text{C}_5\text{Me}_5)_2\text{UH}]_2$, **1** (30 mg, 0.029 mmol), in C_6D_6 . The J-Young tube was capped immediately, and a color change from brown-green to brown-black was observed. ^1H NMR spectroscopy showed quantitative conversion of starting material to the previously characterized **6**,⁵ $(\text{C}_5\text{Me}_5)_2$, and H_2 after 3 days.

$(\text{C}_5\text{Me}_5)_2\text{U}(\text{=NPh})_2$, **7.** PhN=NPh (9 mg, 0.049 mmol) in C_6D_6 was added to a J-Young tube containing $[(\text{C}_5\text{Me}_5)_2\text{UH}]_2$, **1** (25 mg, 0.025 mmol), in C_6D_6 . The J-Young tube was capped immediately, and a color change from brown to brown-red was observed along with the formation of bubbles. ^1H NMR spectroscopy showed quantitative conversion of starting material to the previously characterized **7**,³⁰ and H_2 exhibiting a ^1H NMR resonance at 4.46 ppm.

$(\text{C}_5\text{Me}_5)_2\text{Th}(\text{SPh})_2$, **8.** A pale yellow solution of $(\text{C}_5\text{Me}_5)_2\text{ThCl}_2$ (200 mg, 0.35 mmol) in toluene (10 mL) was added to a white slurry of KSPH (129 mg, 0.87 mmol) in toluene (2 mL), and the

reaction mixture was stirred for 12 h. White insoluble materials were removed by centrifugation, and solvent was removed under reduced pressure to yield **8** as a white, crystalline powder (220 mg, 87%). Crystals of **8** suitable for X-ray diffraction were grown at -35°C from a concentrated toluene solution. ^1H NMR (C_6D_6): δ 2.02 (s, 30H, C_5Me_5 , $\Delta\nu_{1/2} = 1$ Hz), 6.89 (tt, 2H, $^3J_{\text{HH}} = 7$ Hz, *p*-H), 7.04 (tt, 4H, $^3J_{\text{HH}} = 8$ Hz, *m*-H), 7.83 (dd, 4H, $^3J_{\text{HH}} = 8$ Hz, *o*-H). ^{13}C NMR (C_6D_6): δ 12.1 (C_5Me_5), 128.5 (C_5Me_5), 134.0 (*o*-phenyl), 129.2 (*m*-phenyl), 125.3 (*p*-phenyl), 143.0 (*ipso*-phenyl). IR (thin film): 2961s, 2914s, 2856s, 2729w, 2291w, 1579m, 1476m, 1440m, 1378m, 1262s, 1085s, 1065s, 1023s, 803s, 737m, 695s, 664m cm^{-1} . Anal. Calcd for $\text{C}_{32}\text{H}_{40}\text{S}_2\text{Th}$: C, 53.32; H, 5.59; S, 8.90; Th, 32.19. Found: C, 53.22; H, 5.57; S, 8.79; Th, 32.05.

$(\text{C}_5\text{Me}_5)_2\text{Th}(\text{SPh})_2$, **8, from $[(\text{C}_5\text{Me}_5)_2\text{ThH}_2]_2$, **3**.** PhSSPh (10 mg, 0.048 mmol) in C_6D_6 was added to a J-Young tube containing $[(\text{C}_5\text{Me}_5)_2\text{ThH}_2]_2$, **3** (24 mg, 0.024 mmol), in C_6D_6 . The J-Young tube was capped immediately, and a color change from pale yellow to colorless was observed along with the formation of bubbles. ^1H NMR spectroscopy showed quantitative conversion of starting material to **8** and H_2 exhibiting a ^1H NMR resonance at 4.46 ppm.

$[(\text{C}_5\text{Me}_5)(\text{C}_8\text{H}_8)\text{Th}]_2(\text{C}_8\text{H}_8)$, **9.** 1,3,5,7- C_8H_8 (23 μL , 0.203 mmol) was added dropwise to a pale yellow solution of $[(\text{C}_5\text{Me}_5)_2\text{ThH}_2]_2$, **3** (68 mg, 0.067 mmol), in toluene (10 mL). A dark orange solution immediately formed. After the mixture was stirred for 3 days, the dark orange solution was evaporated to dryness, yielding an orange powder. The orange powder was washed with cold hexane (1×5 mL) and dried under reduced pressure to afford **9** (59 mg, 83%). Orange crystals of **9** suitable for X-ray diffraction were grown at 25°C from a concentrated benzene solution. ^1H NMR (C_6D_6 , 25°C): δ 1.93 (s, 30H, C_5Me_5 , $\Delta\nu_{1/2} = 1$ Hz), 6.15 (s, 8H, C_8H_8 , $\Delta\nu_{1/2} = 1$ Hz). ^{13}C NMR (C_6D_6 , 25°C): δ 13.7 (C_5Me_5), 125.9 (C_5Me_5), 99.21 (C_8H_8). ^1H NMR (toluene-*d*₈, 80°C): δ 1.92 (s, 30H, C_5Me_5 , $\Delta\nu_{1/2} = 1$ Hz), 6.06 (s, 8H, C_8H_8 , $\Delta\nu_{1/2} = 1$ Hz). ^1H NMR (toluene-*d*₈, -65°C): δ 1.91 (s, 30H, C_5Me_5 , $\Delta\nu_{1/2} = 1$ Hz), 6.09 (s, 8H, C_8H_8 , $\Delta\nu_{1/2} = 1$ Hz). IR (thin film): 2961s, 2918s, 2856s, 1444m, 1378m, 1258vs, 1089vs, 1085vs, 1015vs, 865s, 803vs, 703s cm^{-1} . Anal. Calcd for $\text{C}_{44}\text{H}_{54}\text{Th}_2$: C, 50.48; H, 5.20. Found: C, 51.20; H, 5.43.

X-ray Data Collection, Structure Determination, and Refinement. **$[(\text{C}_5\text{Me}_5)_2\text{UH}]_2$, **1**.** A black crystal of approximate dimensions $0.15 \times 0.24 \times 0.28$ mm was mounted on a glass fiber and transferred to a Bruker CCD platform diffractometer. The SMART³¹ program package was used to determine the unit-cell parameters and for data collection (25 s/frame scan time for a sphere of diffraction data). The raw frame data were processed using SAINT³² and SADABS³³ to yield the reflection data file. Subsequent calculations were carried out using the SHELXTL³⁴ program. The diffraction symmetry was $2/m$, and the systematic absences were consistent with the centrosymmetric monoclinic space group $P2_1/n$, which was later determined to be correct. The structure was solved by direct methods and refined on F^2 by full-matrix least-squares techniques. The analytical scattering factors³⁵ for neutral atoms were used throughout the analysis. Hydrogen atoms were included using a riding model. There was one molecule of toluene solvent present per formula unit. The hydrides could not be located and were not included in the refinement. At convergence, $wR2 = 0.1054$ and $\text{Goof} = 1.082$ for 855 variables refined against 17 628 data (0.80 \AA). As a comparison for refinement on F , $R1 = 0.0460$ for those 13 375 data with $I > 2.0\sigma(I)$.

(31) SMART Software Users Guide, Version 5.1; Bruker Analytical X-Ray Systems, Inc.; Madison, WI, 1999.

(32) SAINT Software Users Guide, Version 6.0; Bruker Analytical X-Ray Systems, Inc.; Madison, WI, 1999.

(33) Sheldrick, G. M. SADABS, Version 2.10; Bruker Analytical X-Ray Systems, Inc.: Madison, WI, 2002.

(34) Sheldrick, G. M. SHELXTL Version 6.12; Bruker Analytical X-Ray Systems, Inc.; Madison, WI, 2001.

(35) International Tables for X-Ray Crystallography; Kluwer Academic Publishers: Dordrecht, 1992; Vol. C.

(29) Lescop, C.; Arliguie, T.; Lance, M.; Nierlich, M.; Ephritikhine, M. *J. Organomet. Chem.* **1999**, *580*, 137.

(30) Arney, S. J.; Burns, C. J.; Smith, D. C. *J. Am. Chem. Soc.* **1992**, *114*, 10068.

$[(C_5Me_5)_2UH_2]_2$, **2**. A black block $0.17 \times 0.10 \times 0.10$ mm in size was mounted on a Cryoloop with Paratone oil. Data were collected in a nitrogen gas stream at 208(2) K using phi and omega scans. The crystal-to-detector distance was 60 mm and exposure time was 5 s per frame using a scan width of 0.3° . Data collection was 99.9% complete to 25.00° in θ . A total of 13 055 reflections were collected covering the indices $-25 \leq h \leq 13$, $-16 \leq k \leq 17$, $-21 \leq l \leq 19$. A total of 4442 reflections were found to be symmetry independent, with an R_{int} of 0.0305. Indexing and unit cell refinement indicated a C-centered, monoclinic lattice. The space group was found to be $C2/c$ (No. 15). The data were integrated using the Bruker SAINT³² software program and scaled using the SADABS³³ software program. Solution by direct methods (SIR-97) produced a complete heavy-atom phasing model consistent with the proposed structure. All non-hydrogen atoms were refined anisotropically by full-matrix least-squares (SHELXL-97). All hydrogen atoms, with the exception of the hydride hydrogen H1u, were placed using a riding model. Their positions were constrained relative to their parent atom using the appropriate HFIX command in SHELXL-97. The hydride hydrogen H1u was located from the difference map, and its position was refined isotropically.

$(C_5Me_5)_2U(SePh)_2$, **5**. A red plate $0.10 \times 0.10 \times 0.05$ mm in size was mounted on a Cryoloop with Paratone oil. Data were collected in a nitrogen gas stream at 100(2) K using phi and omega scans. A total of 19 076 reflections were collected covering the indices $-17 \leq h \leq 17$, $-17 \leq k \leq 17$, $-42 \leq l \leq 42$. A total of 6385 reflections were found to be symmetry independent, with an R_{int} of 0.0366. Indexing and unit cell refinement indicated a hexagonal lattice. The space group was found to be $P6(1)$ (No. 169). The data were handled as described for **2**. The crystal was a perfect merohedral twin, with a refined BASF parameter of 0.50147(69).

$(C_5Me_5)_2Th(SPh)_2$, **8**. A colorless crystal of approximate dimensions $0.12 \times 0.12 \times 0.21$ mm was handled as described for **1**. The diffraction symmetry was $6/m$, and the systematic absences were consistent with the hexagonal space groups $P6_1$ and $P6_5$. It was later determined that the correct space group was $P6_5$. The structure was solved by direct methods and refined on F^2 by full-matrix least-squares techniques. At convergence, $wR2 = 0.0462$ and $GOF = 1.102$ for 326 variables refined against 7192 data. As a comparison for refinement on F , $R1 = 0.0235$ for those 6673 data with $I > 2.0\sigma(I)$. The absolute structure was assigned by refinement of the Flack parameter.³⁶

$[(C_5Me_5)(C_8H_8)/Th]_2(C_8H_8)$, **9**. An orange crystal of approximate dimensions $0.13 \times 0.17 \times 0.28$ mm was handled as described for **1**. The diffraction symmetry was $2/m$, and the systematic absences were consistent with the monoclinic space group $C2$, Cm , or $C2/m$. It was later determined that the noncentrosymmetric space group $C2$ was correct. The structure was solved using the coordinates of the uranium analogue⁵ and refined on F^2 by full-matrix least-squares techniques. The molecule was located about a 2-fold rotation axis. There was one molecule of benzene solvent present per formula unit. The solvent molecule was also located about a 2-fold axis. At convergence, $wR2 = 0.0716$ and $Gof = 1.034$ for 242 variables refined against 4807 data (0.76 \AA). As a comparison for refinement on F , $R1 = 0.0273$ for those 4489 data with $I > 2.0\sigma(I)$. The absolute structure was assigned by refinement of the Flack parameter.³⁶

Results

Synthesis and Structural Characterization of Uranium Hydrides. The uranium hydrides $[(C_5Me_5)_2UH]_2$, **1**, and $[(C_5Me_5)_2UH_2]_2$, **2**, were originally synthesized by Marks and co-workers from a reaction between $(C_5Me_5)_2UMe_2$ and H_2 that generated a mixture of **1** and **2**, eq 2.¹⁵ The tetravalent hydride,

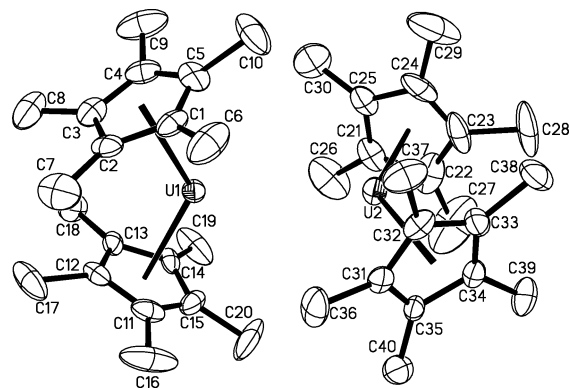


Figure 1. Molecular structure of one of the crystallographically independent molecules in the unit cell of $[(C_5Me_5)_2UH]_2$, **1**, with thermal ellipsoids drawn at the 50% level.

2, is the dominant species under H_2 . However in the absence of hydrogen, **2** loses H_2 to form trivalent **1**. To avoid using mixtures of **1** and **2**, attempts were made to isolate each and confirm their identity by X-ray crystallography.

$[(C_5Me_5)_2UH]_2$, **1**. The conversion of **2** to **1** is facilitated by repeatedly dissolving **2** under argon and removing solvent under vacuum. Hence, removal of solvent from a toluene solution of **2** followed by dissolution in hexane, removal of solvent, and finally dissolution in toluene and removal of solvent generates a brown-green solid that analyzes by 1H NMR spectroscopy in C_6D_6 as a 15:1 mixture of **1**:**2** on the basis of $(C_5Me_5)^-$ resonances. X-ray quality crystals were repeatedly grown from saturated solutions of toluene at $-35^\circ C$ under argon, and a structure was obtained. In contrast to the IR spectrum of **2**,¹⁵ which displays absorptions at 1335 and 1180 cm^{-1} assigned to a terminal U–H stretching mode and a U–H–U stretching mode, respectively, these crystals displayed only a single broad band at 1163 cm^{-1} assignable to a bridging U–H–U stretching mode.

An X-ray crystallographic study revealed a structure containing two similar crystallographically independent molecules in the unit cell, each of which is comprised of two metallocene units as shown in Figure 1.

No hydride ligands were located, but the two metallocenes are presumably bridged by the hydride ligands, as was found in the neutron diffraction study of tetravalent $[(C_5Me_5)_2ThH(\mu-H)]_2$.²⁵ The bimetallic structure is equivalent to that found for $[(C_5Me_5)_2SmH]_2$, **10**,³⁷ another complex in which only the metallocene components were identified by X-ray crystallography. Complex **1**, which crystallized with toluene in the lattice, is not isomorphous with **10**, which crystallized free of solvents.

The spatial arrangement of the four $(C_5Me_5)^-$ ring centroids around the $U\cdots U$ core can be described as a distorted tetrahedron. As shown in Figure 2, the U(2) ion is almost contained within the plane defined by its two ring centroids and U(1). The displacement of this atom is only 0.04 \AA out of this plane. The analogous displacement for U(1) is larger at 0.14 \AA . A similar tetrahedral arrangement was observed in **10**, but with even less distortion.³⁷ In **1**, the $90(8)^\circ$ average (ring centroid)–U–U–(ring centroid) torsional angle is indistinguishable from the $90(4)^\circ$ analogous average in **10**.³⁷ However, the eight analogous (ring centroid)–U–U–(ring centroid) angles for **1** span a wider range, 81.1° to 104.7° , vs 86.7° to 93.3° in **10**.

Each crystallographically independent molecule of **1** has one $128.5\text{--}128.9^\circ$ (C₅Me₅ ring centroid)–U–(C₅Me₅ ring centroid)

(36) Flack, H. D. *Acta Crystallogr., Sect. A* **1983**, *39*, 876–881.

(37) Evans, W. J.; Bloom, I.; Hunter, W. E.; Atwood, J. L. *J. Am. Chem. Soc.* **1983**, *105*, 1401.

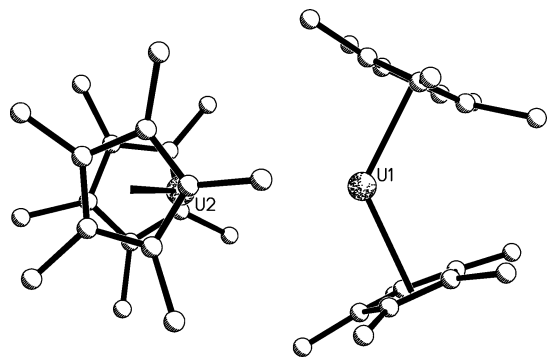


Figure 2. Ball and stick representation of $[(C_5Me_5)_2UH]_2$, **1**.

Table 2. Selected Bond Distances (Å) and Angles (deg) for $[(C_5Me_5)_2UH]_2$, **1**

| | | | |
|----------------|-----------|----------------|-----------|
| U(1)–U(2) | 3.8651(7) | U(3)–U(2) | 3.8530(7) |
| U(1)–C(1) | 2.733(7) | U(2)–C(21) | 2.718(8) |
| U(1)–C(2) | 2.762(8) | U(2)–C(22) | 2.735(9) |
| U(1)–C(3) | 2.791(8) | U(2)–C(23) | 2.740(9) |
| U(1)–C(4) | 2.759(8) | U(2)–C(24) | 2.751(9) |
| U(1)–C(5) | 2.736(7) | U(2)–C(25) | 2.764(8) |
| U(1)–C(11) | 2.748(8) | U(2)–C(31) | 2.747(7) |
| U(1)–C(12) | 2.801(8) | U(2)–C(32) | 2.739(8) |
| U(1)–C(13) | 2.803(7) | U(2)–C(33) | 2.775(8) |
| U(1)–C(14) | 2.768(7) | U(2)–C(34) | 2.811(8) |
| U(1)–C(15) | 2.759(8) | U(2)–C(35) | 2.769(8) |
| U(1)–Cnt1 | 2.482 | U(2)–Cnt3 | 2.469 |
| U(1)–Cnt2 | 2.504 | U(2)–Cnt4 | 2.495 |
| U(3)–Cnt5 | 2.488 | U(4)–Cnt7 | 2.495 |
| U(3)–Cnt6 | 2.497 | U(4)–Cnt8 | 2.489 |
| Cnt1–U(1)–Cnt2 | 128.5 | Cnt3–U(2)–Cnt4 | 133.5 |
| Cnt5–U(3)–Cnt6 | 128.9 | Cnt7–U(4)–Cnt8 | 133.8 |

angle, with the other at 133.5–133.8°. These are in the range typical for f element metallocenes, but the asymmetry is unusual. As shown in Table 2, the U–C(C_5Me_5) bond distances for the two unique molecules in the unit cell have values between 2.718(8) and 2.813(8) Å and average 2.76(2) Å. This average is the same as the 2.76(3) Å analogue in $[(C_5Me_5)_2U(\mu-Cl)]_3$,³⁸ an eight-coordinate U^{3+} metallocene. The four U–(C_5Me_5 ring centroid) distances in **1** are all in the narrow range 2.488–2.497 Å.

The $U\cdots U$ distances for the two unique molecules in **1** are 3.8530(7) and 3.8651(7) Å. In comparison, the $Sm\cdots Sm$ distance in **10** is 3.904 Å. Since the Shannon radius for U^{3+} is 0.067 Å larger than that of Sm^{3+} , the $U\cdots U$ distance in **1** would be expected to be longer. In another similar pair of bridged, eight-coordinate uranium and samarium molecules, the $[(C_5Me_5)_2M(\mu-Cl)]_3$ complexes, the $U\cdots U$ distances averaged 5.669(2) Å compared to 5.633(2) Å for $Sm\cdots Sm$.³⁹ This is in closer agreement to the Shannon radii. The origin of the difference in $M\cdots M$ is not clear, but this is not the first example of a uranium bimetallic complex that differs structurally from a compositionally analogous lanthanide complex. For example, the structure of $[(C_5Me_5)_2U]_2(\mu-O)$ ⁴⁰ differs from that of the $[(C_5Me_5)_2Ln]_2(\mu-O)$ series ($Ln = La, Nd, Sm, Y$)⁴¹ in that the uranium complex contained a 171.5(6)° U–O–U linkage, while the lanthanide complexes had linear, 180° Ln–O–Ln angles.

$[(C_5Me_5)_2UH_2]_2$, **2**. Since **1** is in equilibrium with **2** and since the 1H NMR spectra of samples of **1** in solution contain trace

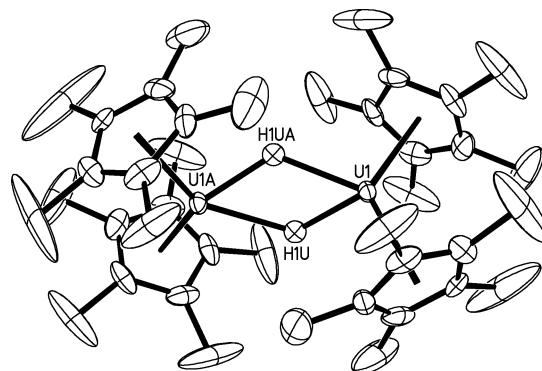


Figure 3. Molecular structure of $[(C_5Me_5)_2UH_2]_2$, **2**, with thermal ellipsoids drawn at the 30% level.

amounts of **2**, it is possible that the crystal described above was the tetravalent uranium hydride **2** and not **1**. To clarify this situation, attempts to get crystallographic data on **2** were made. When the precursor to **1** and **2**, $(C_5Me_5)_2UMe_2$, was placed under 80 psi of H_2 , large crystalline rods could be repeatedly obtained. The 1H NMR spectrum of these crystals matches that reported for $[(C_5Me_5)_2UH_2]_2$, **2**,¹⁵ but over time the spectra showed conversion to $[(C_5Me_5)_2UH]_2$, **1**.

Crystals grown by this procedure diffract X-rays and behave much differently than the crystals of **1**. Repeated attempts to obtain X-ray diffraction data in the typical low-temperature range around 165 K were unsuccessful since the crystals cracked during the data collection. At room temperature, the crystals showed no sign of cracking in the oil used to mount the crystals. Data collection at 238 K avoided the decomposition, but gave data with disorder in the $(C_5Me_5)^-$ rings. Ultimately, data collected at 208 K on a modern instrument that had a shorter data collection time provided the structure shown in Figure 3.

The complex obtained under hydrogen pressure crystallized in the space group $C2/c$, in contrast to the $P2_1/n$ structure of **1**. Like the structure of **1**, the data on **2** show two metallocene units. In this case, there is only one crystallographically independent molecule in the unit cell and the two metallocenes are equivalent by symmetry.

The $U\cdots U$ distance refined to be 3.606(6) Å, Table 3, a distance significantly shorter than the 3.8530(7) and 3.8651(7) Å distances in **1**. This is reasonable considering that the Shannon radius for U^{4+} is 0.135 Å shorter than that for U^{3+} . The $U\cdots U$ distance in **2** is also shorter than the 3.632(2) Å intermetallic distance in the Th^{4+} hydride $[Me_2Si(C_5Me_4)_2ThH_2]_2$.⁴² This difference is in the direction expected on the basis of the nine-coordinate ionic radii of Th^{4+} , 1.09 Å, and U^{4+} , 1.05 Å.⁴³ All of these $An\cdots An$ distances are substantially shorter than the 4.007(8) Å $Th\cdots Th$ distance in $[(C_5Me_5)_2ThH(\mu-H)]_2$, structurally characterized by neutron diffraction,²⁵ but this discrepancy has previously been noted.⁴² The U–C(C_5Me_5) distances in **2** range from 2.729(6) to 2.888(6) Å, a wide range that may reflect the higher than usual data collection temperature. The average, 2.79(5) Å, is similar to that in **1** within error limits, but the ranges of U–C(C_5Me_5) distances for U^{3+} and U^{4+} metallocenes typically overlap.⁴⁴ Despite the complication in the data collection and disorder in the $(C_5Me_5)^-$ ligands, bridging hydrides were located in a difference map and their positions refined isotropically. No terminal hydrides were located.

(38) Manriquez, J. M.; Fagan, P. J.; Marks, T. J. *J. Am. Chem. Soc.* **1979**, *101*, 5075.

(39) Evans, W. J.; Drummond, D. K.; Grate, J. W.; Zhang, H.; Atwood, J. L. *J. Am. Chem. Soc.* **1987**, *109*, 3928.

(40) Evans, W. J.; Kozimor, S. A.; Ziller, J. W. *Polyhedron* **2004**, *23*, 2689.

(41) Evans, W. J.; Davis, B. L.; Nyce, G. W.; Perotti, J. M.; Ziller, J. W. *J. Organomet. Chem.* **2003**, *677*, 89.

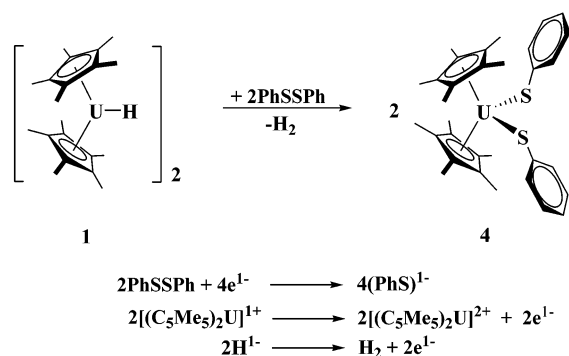
(42) Fendrick, C. M.; Schertz, L. D.; Day, V. W.; Marks, T. J. *Organometallics* **1988**, *7*, 1828.

(43) Shannon, R. D. *Acta Crystallogr., Sect. A* **1976**, *23*, 751.

(44) Evans, W. J.; Miller, K. A.; Ziller, J. W.; Greaves, J. Manuscript in preparation.

Table 3. Selected Bond Distances (Å) and Angles (deg) for [(C₅Me₅)₂UH₂]₂, **2**

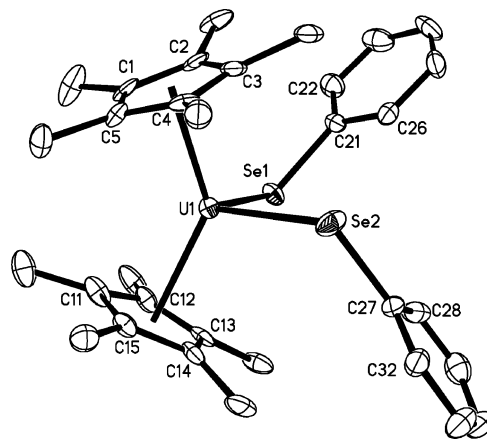
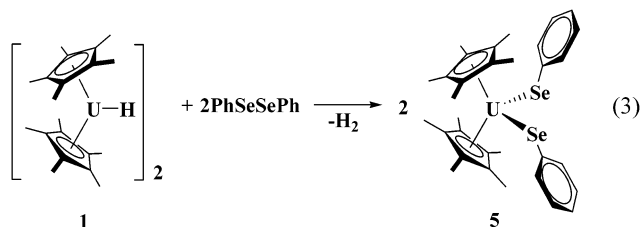
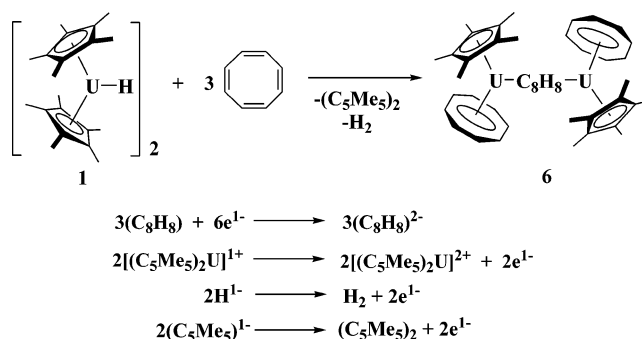
| | |
|----------------|----------|
| U(1)–U(1A) | 3.606(6) |
| U(1)–Cnt1 | 2.499 |
| U(1)–Cnt2 | 2.475 |
| U(1)–C(11A) | 2.867(6) |
| U(1)–C(12A) | 2.809(7) |
| U(1)–C(13A) | 2.794(7) |
| U(1)–C(14A) | 2.843(7) |
| U(1)–C(15A) | 2.888(6) |
| U(1)–C(11B) | 2.755(6) |
| U(1)–C(12B) | 2.754(7) |
| U(1)–C(13B) | 2.738(7) |
| U(1)–C(14B) | 2.729(6) |
| U(1)–C(15B) | 2.739(7) |
| U(1)–H1U | 1.94(9) |
| Cnt1–U(1)–Cnt2 | 127.6 |
| Cnt1–U(1)–H1U | 115.3 |
| Cnt1–U(1)–H1UA | 92.6 |
| Cnt2–U(1)–H1U | 101.0 |
| Cnt2–U(1)–H1UA | 139.5 |

Scheme 3

The structural data that are available as well as the NMR and IR data on the crystals discussed above suggest that these are appropriately assigned as **1** and **2**. It is possible that both crystalline forms are two varieties of just one of these compounds, and it is also possible that the crystals involve mixtures of the two compounds.⁴⁵ However, in terms of their reaction chemistry described next, these crystalline materials behave as **1** and **2** as assigned.

Reductive Chemistry of [(C₅Me₅)₂UH₂]₂, **1.** (C₅Me₅)₂U(SPh)₂, **4**. Addition of trivalent [(C₅Me₅)₂UH₂]₂, **1**, to 2 equiv of PhSSPh in C₆D₆ in a J-Young NMR tube caused an immediate brown to red color change and the evolution of gas. ¹H NMR spectroscopy revealed quantitative formation of the previously reported (C₅Me₅)₂U(SPh)₂, **4**,²⁹ which has a (C₅Me₅)[−] ¹H NMR resonance at 13.2 ppm. A ¹H NMR resonance at 4.46 ppm consistent with H₂ was also observed. Overall, this is a four-electron reduction, with two electrons formally from the U³⁺ ions in **1** and two electrons from the two H[−] ligands, Scheme 3. PhSSPh has a reduction potential of −1.6 V vs Ag/AgNO₃.⁴⁶

(C₅Me₅)₂U(SePh)₂, **5**. Complex **1** reacts similarly with 2 equiv of PhSeSePh, which has a reduction potential of −0.9 V vs Ag/AgNO₃,⁴⁶ to form (C₅Me₅)₂U(SePh)₂, **5**, and H₂, eq 3. Red crystals of **5** were isolated in 67% yield and displayed a (C₅Me₅)[−] ¹H NMR resonance at 14.0 ppm. Definitive identi-

**Figure 4.** Molecular structure of (C₅Me₅)₂U(SePh)₂, **5**, with thermal ellipsoids drawn at the 50% probability level.**Scheme 4**

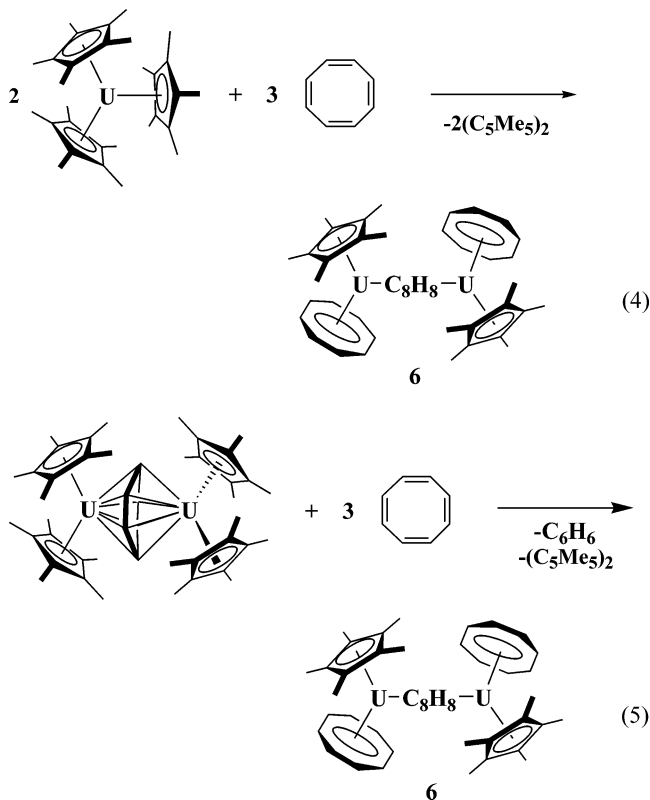
fication of **5** was obtained by X-ray crystallography, Figure 4. Again, this is a four-electron reduction, Scheme 3.

[(C₅Me₅)(C₈H₈)U]₂(C₈H₈), **6**. Complex **1** reduces 3 equiv of 1,3,5,7-C₈H₈ to quantitatively form the previously reported brown crystalline complex [(C₅Me₅)(C₈H₈)U]₂(C₈H₈), **5**.⁵ The byproducts observed by ¹H NMR spectroscopy were H₂ and (C₅Me₅)₂, Scheme 4. This transformation requires that [(C₅Me₅)₂UH₂]₂ deliver six electrons. These can be accounted for as shown in Scheme 4. Two electrons arise from two U³⁺ ions and two electrons are generated from the two hydrides, as shown in Scheme 3. However, in this reaction, two additional electrons arise from two (C₅Me₅)[−] ions, presumably from sterically induced reduction involving a crowded intermediate. Sterically induced reduction has been involved in each previous synthesis of **6**,^{5,8} eqs 4 and 5. The first and second reduction potentials of C₈H₈ are −1.85 and −1.9 V vs SCE.⁴⁷

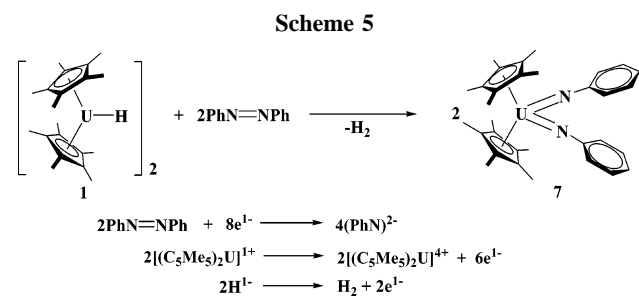
(C₅Me₅)₂U(=NPh)₂, **7**. In an attempt to determine if the reducing power of the hydride ligands in **1** could be combined with a U³⁺ to U⁶⁺ redox change, **1** was added to 2 equiv of PhN=NPh. After 12 h, quantitative formation of the previously characterized U⁶⁺ bis(imido) complex (C₅Me₅)₂U(=NPh)₂,^{6,30} **7**, was observed along with H₂, Scheme 5. In this case, the overall reaction involved an eight-electron reduction. As shown in Scheme 5, each hydride delivers one electron as each U³⁺ provides three.

Reductive Chemistry of [(C₅Me₅)₂UH₂]₂, **2.** Examining the reactivity of the hydride ligands in tetravalent **2** is more complicated because in solution it converts to trivalent **1** and hydrogen, eq 2. However, since the molecular weights of **1** and **2** differ by only 2 Da, it is possible to get the stoichiometry

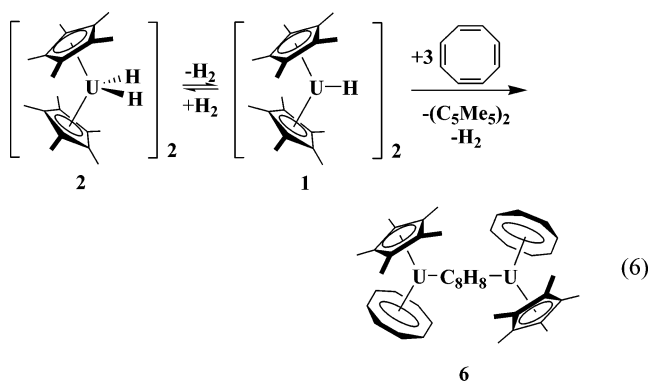
(45) Parkin, G. *Acc. Chem. Res.* **1992**, *25*, 455.(46) Dessy, R. E.; Weissman, P. M.; Pohl, R. L. *J. Am. Chem. Soc.* **1966**, *88*, 5117.(47) de Boer, E. *Adv. Organomet. Chem.* **1964**, *2*, 115.



close to that needed for reduction by either uranium reagent. Since the synthesis of **2** from $(C_5Me_5)_2U-Me_2$ and H_2 at 1 atm typically provides **2** as a 50% mixture with **1**, this is the material that was used to evaluate tetravalent uranium hydride reduction. With PhSSPh, PhSeSePh, C_8H_8 , and PhN=NPh, the same products described in Schemes 3–5 and eq 3 above, namely,



4–**7**, respectively, were observed in reactions with the mixture of **1** and **2**. Equation 6 shows one example. Operationally, this

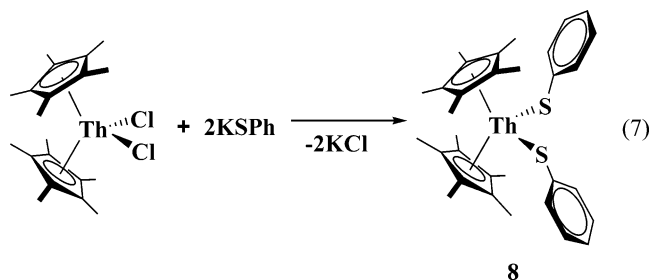


means that either the tetravalent or trivalent uranium hydrides can be used in these reductions. Mechanistically, it is possible

that all of these reductions occurred via trivalent **1**. As the concentration of **1** gets depleted, more **2** could convert to **1** via eq 1.

Reductive Chemistry of $[(C_5Me_5)_2ThH_2]_2$, **3.** To examine reductive tetravalent actinide chemistry without the complication of the equilibrium between **1** and **2**, reduction reactions with the tetravalent thorium hydride **3**¹⁵ were examined. In this case, there is no evidence of a similar tetravalent to trivalent conversion.¹⁵ In contrast to organometallic uranium chemistry,² examples of Th^{3+} complexes are very rare.^{16–19}

Initially, the reductive reactivity of $[(C_5Me_5)_2ThH_2]_2$, **3**, was examined with PhSSPh. Reaction of **3** with 2 equiv of PhSSPh in a J-Young tube led to gas evolution and quantitative conversion to a product, **8**, that displayed a single $(C_5Me_5)^-$ resonance in the 1H NMR spectrum at 2.02 ppm as well as three unique phenyl resonances. A resonance at 4.46 ppm consistent with H_2 was also observed in the 1H NMR spectrum. The identity of **8** was determined by independent synthesis from $(C_5Me_5)_2ThCl_2$ and KSPH, as shown in eq 7. This is analogous



to the synthesis of $(C_5Me_5)_2U(SPh)_2$.²⁹ Definitive characterization of **8** was accomplished by X-ray crystallography, Figure 5. Hence, **3** reacts with PhSSPh according to Scheme 6 in a

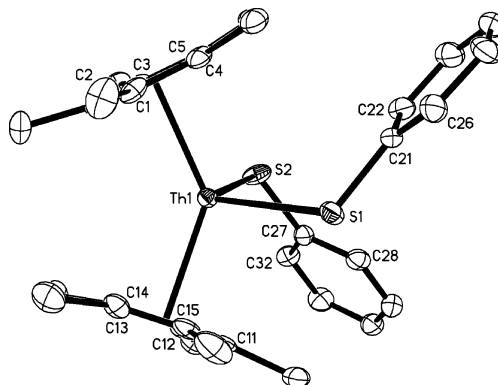
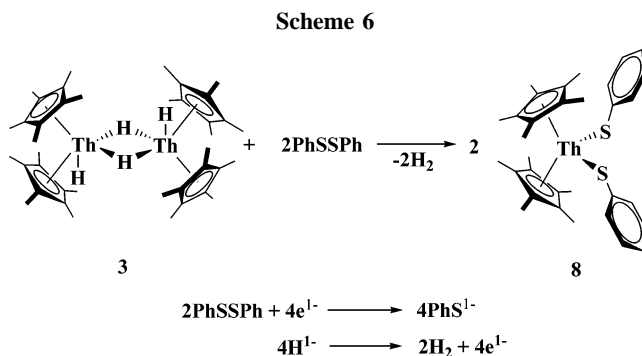


Figure 5. Molecular structure of $(C_5Me_5)_2Th(SPh)_2$, **8**, with thermal ellipsoids drawn at the 50% probability level.

reaction analogous to Scheme 3. However, in this case the reduction is due entirely to the hydride ligands, as shown in Scheme 6.



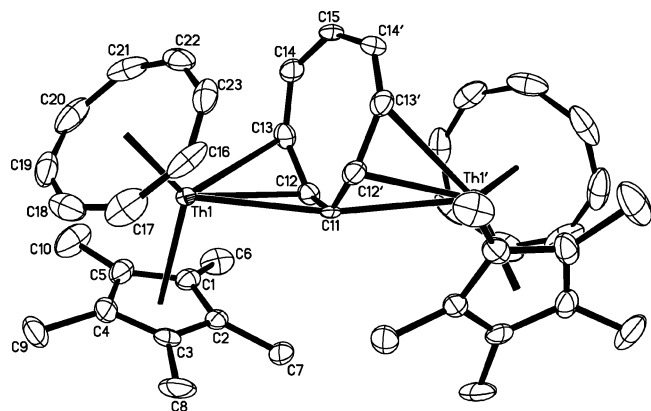


Figure 6. Molecular structure of $[(C_5Me_5)(C_8H_8)Th]_2(C_8H_8)$, **9**, with thermal ellipsoids drawn at the 50% probability level.

Scheme 7

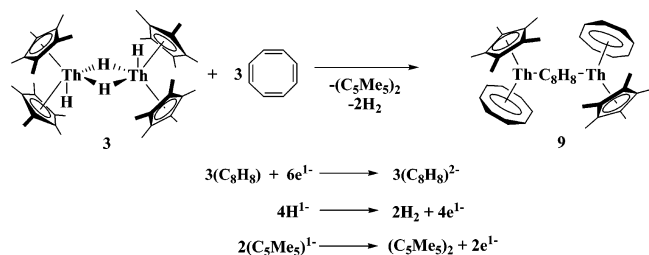


Table 4. Selected Bond Distance (Å) and Angles (deg) for $(C_5Me_5)_2U(SePh)_2$, **5**, and $(C_5Me_5)_2Th(SPh)_2$, **8**

| | 5 M = U; E = Se | 8 M = Th; E = S |
|-----------------|---------------------------|---------------------------|
| M(1)–E(1) | 2.8011(7) | 2.7488(11) |
| M(1)–E(2) | 2.7997(7) | 2.7451(10) |
| M(1)–Cnt1 | 2.459 | 2.525 |
| M(1)–Cnt2 | 2.463 | 2.525 |
| E(1)–C(21) | 1.926(6) | 1.769(4) |
| E(2)–C(27) | 1.911(6) | 1.774(4) |
| Cnt1–M(1)–E(1) | 112.8 | 111.3 |
| Cnt1–M(1)–E(2) | 95.5 | 95.0 |
| Cnt2–M(1)–E(1) | 94.3 | 95.8 |
| Cnt2–M(1)–E(2) | 111.1 | 113.0 |
| Cnt1–M(1)–Cnt2 | 137.3 | 135.5 |
| C(21)–E(1)–M(1) | 112.74(17) | 113.76(13) |
| C(27)–E(2)–M(1) | 114.8(2) | 114.74(14) |
| E(1)–M(1)–E(2) | 101.77(2) | 103.00(3) |

$[(C_5Me_5)(C_8H_8)Th]_2(C_8H_8)$, **9**. In an attempt to make an analogue of **6**, complex **3** was reacted with 3 equiv of C_8H_8 . Over a period of 3 days, light orange crystalline $[(C_5Me_5)(C_8H_8)Th]_2(C_8H_8)$, **9**, was formed in >80% yield. This product was fully characterized by X-ray crystallography, Figure 6. The 1H NMR spectrum of **9** showed only two resonances at 1.93 and 6.15 ppm compared to three resonances at 5.5, –41.7, and –42.2 ppm in paramagnetic **6**. Only a single C_8H_8 resonance was observed for **9** down to –65 °C. In this case, a six-electron reduction was accomplished by combining hydride reduction with $(C_5Me_5)^-$ reduction, presumably from a sterically crowded intermediate, Scheme 7. This is supported by the fact that $(C_5Me_5)_2$, the signature byproduct of sterically induced reduction, was observed in the 1H NMR spectrum. This is the first evidence of sterically induced reduction chemistry with thorium.⁴⁸

Structural Studies of Reduction Products. The X-ray crystal structures of $(C_5Me_5)_2U(SePh)_2$, **5**, and $(C_5Me_5)_2Th(SPh)_2$, **8**, display conventional metallocene bonding parameters for formally eight-coordinate tetravalent complexes of this type as shown in Table 4. The Th– (C_5Me_5) ring centroid) distances are approximately 0.05 Å longer than the uranium values, consistent with the 0.05 Å difference in the Shannon ionic radii

for eight-coordinate U^{4+} and Th^{4+} .⁴³ The difference in actinide–chalcogen bonds, An–E, also matches the differences in the radii of the components. With the selenium distances expected to be 0.14 Å longer and uranium lengths 0.05 Å shorter, the U–Se distance should be 0.09 Å longer than the Th–S distance on the basis of Shannon radii. Comparison of the 2.801(1) and 2.780(1) Å U–Se distances in **5** and the 2.749(1) and 2.745(1) Å Th–S distances in **8** gives the expected trend, but the 0.05 Å difference is not as large. If this represents any real difference in An–E bonding interactions, it is not reflected in the An–E–C(*ipso*) angles, which fall in the narrow range 112.7(2)–114.8(2)°. In the $(C_5Me_5)_2Sm(EPh)(THF)$ series, the Sm–E–C(*ipso*) angles are also similar: 120.82(17)° for E = S and 118.51(14)° for E = Se.²⁷ The 0.137–0.157 Å difference in the E–C(Ph) distances in **5** and **8** also matches the 0.14 Å difference in sulfur and selenium size.

The structure of $[(C_5Me_5)(C_8H_8)Th]_2(C_8H_8)$, **9**, is isomorphous with that of $[(C_5Me_5)(C_8H_8)U]_2(C_8H_8)$, **6**. As shown in Table 5, the actinide carbon distances are larger in **9**, as expected for the larger metal, thorium. The structure of **6** was unusual in that it contains a nonplanar $(C_8H_8)^{2-}$ dianion. This $(C_8H_8)^{2-}$ bridges the two uranium atoms with a pseudo-allyl orientation to each. These two allyl units show a common atom, C(11). Interestingly, this is not a unique structure for uranium, but it is found also in the thorium structure. Although An–C(12) is longer for thorium than for uranium as expected, the An–C(11) and An–C(13) distances are shorter for thorium. The uranium complex **6** also has a broader range of An–C(pseudo-allyl) distances, 2.687(1)–3.00(2) Å, compared to thorium, 2.731(6)–2.933(6) Å. The consequences of these structural features on reactivity are under investigation.

Discussion

Trivalent Uranium Hydrides as Multielectron Reductants.

The reduction chemistry in Schemes 3–5 and eq 3 shows that the hydride ligands in solutions containing a high proportion of the sterically normal complex $[(C_5Me_5)_2UH]_2$, **1**, can function as effective reducing agents and combine with U^{3+} to effect multielectron reduction reactions. Solutions of bimetallic **1** have been shown to accomplish four-, six-, and eight-electron reductions depending on the substrate. In each case, H_2 is a byproduct. Hence, the hydride ligand reacts cleanly to deliver an electron according to eq 1 without complications of insertion or σ bond metathesis chemistry. With the PhSSPh and PhSeSePh substrates, Scheme 3 and eq 3, the four-electron reductions involve a simple combination of two H^-/H and two U^{3+}/U^{4+} redox couples. In the case of the six-electron reduction of 3 equiv of C_8H_8 , Scheme 4, these hydride- and U^{3+} -based reductions appear to combine with sterically induced reduction involving two $(C_5Me_5)^-$ ligands since $(C_5Me_5)_2$ is a byproduct. The eight-electron reduction in Scheme 5 shows that the hydride-based reduction can also combine with U^{3+} to U^{6+} redox processes.

Tetravalent Uranium Hydrides. The small amount of tetravalent $[(C_5Me_5)_2UH_2]_2$, **2**, contained in the solutions of **1** due to the equilibrium in eq 2 did not affect the success of the reductions above. In fact, it appears that **2** is an equally effective reductant. Hence, the 1:1 samples of **1** and **2** also effect the reductions described above. Although each of the reactions done with these mixtures could proceed through **1**, the reductive capacity of the tetravalent thorium analogue, $[(C_5Me_5)_2ThH_2]_2$, **3**, suggests that the hydride ligands in **2** could also be one-electron reductants. In this sense, the four hydride ligands in **2**

(48) Evans, W. J.; Nyce, G. W.; Ziller, J. W. *Organometallics* **2001**, *20*, 5489.

Table 5. Selected Bond Distances (Å) and Angles (deg) for [(C₅Me₅)(C₈H₈)Th]₂(C₈H₈), **9**, and [(C₅Me₅)(C₈H₈)U]₂(C₈H₈), **6**⁵

| | [(C ₅ Me ₅)(C ₈ H ₈)Th] ₂ (C ₈ H ₈) 9 | [(C ₅ Me ₅)(C ₈ H ₈)U] ₂ (C ₈ H ₈) 6 |
|---|---|--|
| M(1)–C(11) | 2.8495(11) | 2.878(2) |
| M(1)–C(12) | 2.731(6) | 2.687(17) |
| M(1)–C(13) | 2.933(6) | 3.00(2) |
| M(1)–Cnt1(C ₅ Me ₅) | 2.575 | 2.552 |
| M(1)–Cnt2(C ₈ H ₈) | 2.058 | 1.984 |
| (C ₅ Me ₅)Cnt1–M(1)–C(11) | 98.6 | 99.7 |
| (C ₅ Me ₅)Cnt1–M(1)–C(12) | 90.3 | 92.4 |
| (C ₅ Me ₅)Cnt1–M(1)–C(13) | 102.9 | 104.6 |
| (C ₈ H ₈)Cnt2–M(1)–C(11) | 123.6 | 119.8 |
| (C ₈ H ₈)Cnt2–M(1)–C(12) | 137.6 | 133.1 |
| (C ₈ H ₈)Cnt2–M(1)–C(13) | 119 | 116.5 |
| (C ₅ Me ₅)Cnt1–M(1)–Cnt2(C ₈ H ₈) | 132.1 | 134.5 |
| C(11)–M(1)–C(13) | 53.30(15) | 53.3(6) |
| C(12)–M(1)–C(13) | 28.63(16) | 28.4(6) |
| C(12)–M(1)–C(11) | 29.35(14) | 29.2(6) |
| M(1)′–C(11)–M(1) | 168.4(2) | 172.1(12) |
| M–C(C ₅ Me ₅) range | 2.813(6)–2.864(6) | 2.782(16)–2.811(18) |
| M–C(C ₈ H ₈) range | 2.702(6)–2.777(6) | 2.62(2)–2.723(19) |

provide reduction capacity equivalent to the two hydrides and the two U³⁺ ions in **1**.

Tetravalent Thorium Hydrides. Schemes 6 and 7 show that [(C₅Me₅)₂ThH₂]₂, **3**, can function as a four- and six-electron reductant, respectively, and accomplish reduction analogous to that of trivalent [(C₅Me₅)₂UH]₂, **1**, and tetravalent [(C₅Me₅)₂-UH₂]₂, **2**. The reduction of 2 equiv of PhSSPh to four (SPh)[−] ligands in Scheme 6 apparently is effected only by hydride ligands. In Scheme 7, these four hydrides appear to combine their reduction chemistry with sterically induced reduction to allow **3** to deliver six electrons overall. It is possible that these reactions involve a Th³⁺ intermediate formed by hydride reduction of Th⁴⁺ in analogy with eq 2, but so far no evidence of a Th³⁺ intermediate has been observed. Indeed, the paucity of Th³⁺ complexes^{16–19} is the reason that this hydride-based thorium chemistry is so important to this element. The extensive reduction chemistry available through U³⁺² has not been accessible in thorium compounds. Only when external alkali metal reductants have been added to Th⁴⁺ precursors has reductive chemistry been possible.^{16,20–24} In the case of [(C₅Me₅)₂ThH₂]₂, **3**, the reductants are an integral part of the Th⁴⁺ complex and the byproduct is an easily separated gas, H₂.

The reactions of **3** suggest that much of the reductive trivalent chemistry of U³⁺ can be extended to thorium for the first time. For example, [(C₅Me₅)(C₈H₈)U]₂(C₈H₈), **6**, can be formed in several ways from U³⁺ starting materials, e.g., eqs 4 and 5, but there were no analogous Th³⁺ precursors for [(C₅Me₅)(C₈H₈)Th]₂(C₈H₈), **9**. Since the hydride ligands in **3** are effective reductants, complexes such as **9** can now be generated for thorium.

Synthetic Considerations. Since both [(C₅Me₅)₂UH]₂, **1**, and [(C₅Me₅)₂UH₂]₂, **2**, are synthetically easier to access than the sterically crowded (C₅Me₅)₃U and [(C₅Me₅)₂U]₂(C₆H₆), complexes **1** and **2** become the reagents of choice to make products like those shown in Schemes 3–5 and eq 3. The synthesis of [(C₅Me₅)(C₈H₈)U]₂(C₈H₈), **6**, in particular is now much easier. This should open up this complex and its thorium analogue for comparative reactivity studies for the first time.

Another important difference between **1** and **2** and complexes like (C₅Me₅)₃U and [(C₅Me₅)₂U]₂(C₆H₆) is that the reduction equivalents in **1** and **2** are derived from H₂ according to eq 2. The other compounds require alkali metal reduction in their synthesis. In terms of developing catalytic or at least cyclic

versions of organoactinide-based reduction reactions, it is easier to envisage cycles involving H₂ rather than alkali metals as the stoichiometric reductant.

In general, it appears that any time a synthetic route to a new actinide complex is needed, hydride complexes should be considered as precursors. It is unlikely that the actinide hydrides will cleanly effect reduction and release of H₂ in every process, but certainly the substrates used in this paper demonstrate that this is possible. The facile reductions with actinide hydrides observed here suggest that a broader investigation of electro-positive metal hydride reductions is appropriate. For example, the trivalent lanthanide hydrides such as [(C₅Me₅)₂LnH]₂ may be equivalently useful as reducing agents.

Conclusion

Efficient ways to make solutions containing a high proportion of [(C₅Me₅)₂UH]₂, **1**, have been developed that allow the reductive chemistry of this trivalent hydride to be defined. This complex can accomplish four-, six-, and eight-electron reductions depending on the substrate. The related tetravalent complex [(C₅Me₅)₂UH₂]₂, **2**, can effect analogous reductions in which all of the reduction equivalents arise from the hydride ligands. Extension of this chemistry to [(C₅Me₅)₂ThH₂]₂, **3**, provides a method for thorium reduction chemistry to be effected without requiring the synthesis of a Th³⁺ precursor or addition of an external reductant.

More generally, this study shows that the ligand-based reduction chemistry previously observed with f element complexes of (C₅Me₅)[−] ligands in sterically crowded environments and in (BPh₄)[−] compounds can be extended to other ligands common in f element complexes. The hydride case reported here may just be one example of many to be discovered in the future.

Acknowledgment. We thank the National Science Foundation for support of this research.

Supporting Information Available: X-ray diffraction details (CIF) and X-ray data collection, structure solution, and refinement of compounds **1**, **2**, **5**, **6**, **8**, and **9** (PDF). This material is available free of charge via the Internet at <http://pubs.acs.org>.

OM7003139